Attenuation of Interstitial Fibrosis and Tubular Apoptosis in db/db Transgenic Mice Overexpressing Catalase in Renal Proximal Tubular Cells

Marie-Luise Brezniceanu,[1] Fang Liu,[1] Chih-Chang Wei,[1] Isabelle Chénier,[1] Nicolas Godin,[1] Shao-Ling Zhang,[1] Janos G. Filep,[2] Julie R. Ingelfinger,[3] and John S.D. Chan[1]

OBJECTIVE—The present study investigated the relationships between reactive oxygen species (ROS), interstitial fibrosis, and renal proximal tubular cell (RPTC) apoptosis in type 2 diabetic *db/db* mice and in *db/db* transgenic (Tg) mice overexpressing rat catalase (rCAT) in their RPTCs (*db/db* rCAT-Tg).

RESEARCH DESIGN AND METHODS—Blood pressure, blood glucose, and albuminuria were monitored for up to 5 months. Kidneys were processed for histology and apoptosis studies (terminal transferase-mediated dUTP nick-end labeling or immunostaining for active caspase-3 and Bax). Real-time quantitative PCR assays were used to quantify angiotensinogen (ANG), p53, and Bax mRNA levels.

RESULTS—db/db mice developed obesity, hyperglycemia, hypertension, and albuminuria. In contrast, *db/db* rCAT-Tg mice became obese and hyperglycemic but had normal blood pressure and attenuated albuminuria compared with *db/db* mice. Kidneys from *db/db* mice displayed progressive glomerular hypertrophy, glomerulosclerosis, interstitial fibrosis, and tubular apoptosis and increased expression of collagen type IV, Bax, and active caspase-3, as well as increased ROS production. These changes, except glomerular hypertrophy, were markedly attenuated in kidneys of *db/db* rCAT-Tg mice. Furthermore, ANG, p53, and Bax mRNA expression was increased in renal proximal tubules of *db/db* mice but not of *db/db* rCAT-Tg mice.

CONCLUSIONS—Our results indicate a crucial role for intrarenal ROS in the progression of hypertension, albuminuria, interstitial fibrosis, and tubular apoptosis in type 2 diabetes and demonstrate the beneficial effects of suppressing ROS formation. ***Diabetes*** **57:451–459, 2008**

From the [1]Université de Montréal, Centre hospitalier de l'Université de Montréal (CHUM) Hôtel-Dieu, Research Centre, Pavillon Masson, Montreal, Quebec, Canada; the [2]Université de Montréal, Maisonneuve-Rosemont Hospital, Research Centre, Montreal, Quebec, Canada; and the [3]Pediatric Nephrology Unit, Harvard Medical School, Massachusetts General Hospital, Boston, Massachusetts.

Address correspondence and reprint requests to John Chan, Université de Montréal, Centre hospitalier de l'Université de Montréal (CHUM) Hôtel-Dieu, Research Centre, Pavillon Masson, 3850 Saint Urbain St., Montreal, Quebec, Canada H2W 1T8. E-mail: john.chan@umontreal.ca.

Received for publication 3 February 2007 and accepted in revised form 26 October 2007.

Published ahead of print at http://diabetes.diabetesjournals.org on 31 October 2007. DOI: 10.2337/db07-0013.

Ang, angiotensin; ANG, angiotensinogen; CAT, catalase; ECM, extracellular matrix; KAP, kidney androgen-regulated promoter; mRPT, mouse renal proximal tubule; RAS, renin-angiotensin system; rCAT, rat catalase; ROS, reactive oxygen species; RPTC, renal proximal tubular cell; TGF-β1, transforming growth factor-β 1; TUNEL, transferase-mediated dUTP nick-end labeling.

Diabetes affects 5–10% of the world population. It is estimated that 30–40% and 5–10% of patients with type 1 and type 2 diabetes, respectively, will eventually develop kidney failure or end-stage renal disease (1). Diabetic nephropathy is now the most common cause of end-stage renal disease, accounting for 40–50% (2). Diabetic nephropathy is associated with an increased risk of hypertension, myocardial infarction, stroke, and cardiovascular dysfunction (3). Multiple factors have been implicated in the pathogenesis of diabetic nephropathy, including hyperglycemia, hypertension, insulin resistance, and oxidative stress (4). However, the molecular mechanisms of action of these risk factors are incompletely understood.

Oxidative stress has long been implicated in the progression of diabetes complications. High glucose induces reactive oxygen species (ROS) generation, and ROS contribute to apoptosis in podocytes and mesangial and tubular cells (5–7). Ang II stimulates ROS generation via heightened NADPH oxidase activity in various renal cell types, whereas antioxidants provide renal protection in part by ameliorating oxidative stress (8–11). Such data strongly indicate a link between ROS, renin-angiotensin system (RAS) activation, and renal cell apoptosis in diabetes.

Recent studies have reported that 71% of glomeruli from proteinuric type 1 diabetic patients have glomerulo-tubular junction abnormalities, including atubular glomeruli, which may occur in 8–17% of nephrons (12,13). Atubular glomeruli, glomeruli that are not connected to their proximal tubules as an end result of tubular atrophy, are characteristic of a variety of human kidney diseases including diabetic nephropathy (rev. in 14). Indeed, tubular atrophy appears to be a better predictor of renal disease progression than glomerular pathology because of its close association with loss of renal function (11,15–17).

The mechanisms underlying tubular atrophy remain to be defined. One attractive mechanism is apoptosis. Indeed, apoptotic cell death was detected in a number of renal diseases (18–21). For instance, renal proximal tubular cells (RPTCs) exhibit apoptosis in streptozotocin-induced diabetic mice (22–24) and rats (25,26), as well as in diabetic patients (27,28), suggesting that tubular apoptosis might precede tubular atrophy in atubular glomeruli.

We have reported previously that high glucose evokes ROS generation and enhances angiotensinogen (ANG) (the sole substrate of RAS) gene expression in rat RPTCs (29). The present study investigated whether catalase (CAT) overexpression in RPTCs attenuates the high-glucose action on interstitial fibrosis and tubular apoptosis, ANG,

and proapoptotic gene (p53, Bax, and caspase-3) expression in type 2 diabetic *db/db* mice in vivo. For this purpose, we created *db/db* transgenic (Tg) mice overexpressing rat catalase (rCAT) in RPTCs (*db/db* rCAT-Tg) by crossbreeding heterozygous db/m$^+$ mice with our established homozygous Tg mice overexpressing rCAT in RPTCs (24).

RESEARCH DESIGN AND METHODS

Reagents. Rabbit polyclonal antibodies against bovine CAT and monoclonal antibodies against β-actin were purchased from Sigma-Aldrich Canada (Oakville, ON, Canada). Anti-cleaved caspase-3 polyclonal antibody, anti-Bax polyclonal antibody, and monoclonal anti-collagen type IV antibody were obtained from New England Biolabs (Pickering, ON, Canada), Santa Cruz Biotechnologies (Santa Cruz, CA), and Chemicon International (Temecula, CA), respectively. rCAT cDNA was a gift from Dr. Paul E. Epstein (University of Louisville, Louisville, KY). pKAP2 plasmid containing the kidney-specific androgen-regulated protein (KAP) promoter responsive to testosterone stimulation was obtained from Dr. Curt Sigmund (University of Iowa, Iowa, IA) and has been described elsewhere (30). Placebo pellets or pellets containing 5 mg testosterone with a 91-day release schedule (Cat. #NA-151) were purchased from Innovative Research of America (Sarasota, FL). Oligonucleotides were synthesized by Invitrogen (Burlington, ON, Canada). Restriction and modifying enzymes were from either Invitrogen, La Roche Biochemicals (Dorval, QC, Canada), or Amersham-Pharmacia Biotech (Baie d'Urfé, QC, Canada).

Generation of db/db rCAT-Tg Mice. Tg mice (C57Bl/6 background) overexpressing rCAT in RPTCs (line #688) were created in our lab (by J.S.D.C) and have been described previously (24). Homozygous rCAT-Tg mice were then crossed with heterozygous db/m$^+$ mice (B6.Cg $m^{+/+}$ $Lepr^{db}$ in C57BL/6J background) (Jackson Laboratories, Bar Harbor, ME). Breeding was continued until homozygous *db/db* rCAT-Tg mice were obtained. db/db mice (B6.Cg + $Lepr^{db/+}$ $Lepr^{db/+}$ on a C57BL/6J background) were also purchased from Jackson Laboratories with a specific request for animals with persistent hyperglycemia. The blood glucose levels on arrival were >20 and >25 mmol/l glucose for female and male *db/db* mice, respectively. These levels were maintained throughout the experimental periods until 20 weeks of age. Homozygous *db/db* rCAT-Tg mice were identified by the PCR of genomic DNA for the rCAT transgene (24) and the mutated leptin receptor gene (31). The rCAT sense primer 5′-AAGCGGCCGCATGGCGGACAGCCGGGACCC-3′ and the HA (a tag sequence encoding amino acid residues 98–106 [YPYDVPDYA] of human influenza virus hemagglutinin) anti-sense primer 5′-GGCGTAGTCAGGCACGTCGT-3′ (32), the mouse leptin receptor gene forward primer 5′-AGAACGGACACTCTTTGAAGTCTC-3′ and the reverse primer 5′-CATTCAAACCATAGTTTAGGTTTGTGT-3′ of the mouse leptin receptor gene (31), respectively, were used for PCR. The DNA fragment (135 bp) of mouse leptin receptor gene was then digested with the restriction enzyme *Rsa*I for 1 h at 37°C. If the allele was mutated, the 135-bp DNA fragment was cut into two smaller DNA fragments, appearing as 106- and 29-bp DNA fragments on 3% agarose gel electrophoresis.

Six to eight mice at 20 weeks of age were studied per group. Non-Tg age- and sex-matched db/m$^+$ littermates served as controls. Females were implanted at week 8 with testosterone pellets (5 mg testosterone under 91-day release) or placebo pellets. All animals received standard mouse diet and water ad libitum. Animal care met the standards set forth by the Canadian Council on Animal Care, and all procedures were approved by the CHUM Animal Care Committee.

Experimental protocol. Blood pressure was monitored with a BP-2000 tail-cuff pressure instrument (Visitech Systems, Apex, NC) every 2 weeks for a period of 12 weeks, starting at age 8 weeks, measured three to four times per week and averaged. Each mouse was trained for at least for 5 consecutive days (30–60 min of blood pressure measurements) before the first study blood pressure measurements. Body weight was recorded, and blood glucose level was quantified weekly with an ACCU-CHEK Compact Plus glucose meter (Roche Diagnostics, Laval, QC, Canada). The mice were housed in metabolic cages to obtain 24-h urine samples for the assessment of albuminuria by ELISA (Albuwell and Creatinine companion; Exocell, Philadelphia, PA) (24,32). At the indicated times, the animals were killed by CO_2, and their kidneys were removed immediately. The left kidney was used for histology and immunohistochemistry. The right kidney was used for proximal tubule isolation by Percoll gradient (24,33). Aliquots of freshly isolated mouse renal proximal tubules (mRPTs) were immediately used for protein extraction or total RNA isolation.

Western blot analysis. Western blot analysis was performed as described previously (24,33). The membrane was first blotted with rabbit anti-CAT and then re-blotted with anti–β-actin monoclonal antibodies and chemiluminescent developing reagent (La Roche Biochemicals). The relative densities of CAT and β-actin bands were quantified by computerized laser densitometry (ImageQuant software, version 5.1; Molecular Dynamics).

ROS generation. Aliquots of freshly isolated proximal tubules were immediately used for ROS measurement by the lucigenin method (24,33). ROS production in mRPTs was normalized with protein concentration and expressed as relative light units per microgram of protein.

Morphological studies. Kidneys were collected in Tissue-Tek cassettes (VWR Canlab, Montreal, QC, Canada), dipped immediately in ice-cold formaldehyde (10% in PBS) and fixed for 24 h at 4°C. The cassettes were then processed by the CHUM Pathology Department. Tissue sections (four to five specimens per group) were stained with periodic acid schiff or Masson's trichrome and analyzed visually under a light microscope by an observer unaware of the treatments. The collected images were analyzed and quantified using NIH ImageJ software.

The mean glomerular volume (V_G) was determined by the method of Weibel (34) with the aid of an image analysis software system (Motics Images Plus 2.0; Motic, Richmond, BC, Canada). The V_G was estimated by the mean glomerular tuft area (A_T) derived from the light microscopic measurement of 30 random sectional profiles of glomeruli from each group ($n = 6$ animals per group) using the formula: $V_g = \beta/k \times A_T^{1.5}$, where $\beta = 1.382$ (shape coefficient for spheres) and $k = 1.1$ (size distribution coefficient).

Terminal transferase-mediated dUTP nick-end labeling assay and immunohistochemical staining. Formaldehyde-fixed, paraffin-embedded kidney sections (5-μm thick) were deparaffinized in xylene and rehydrated. Apoptosis was assessed with a transferase-mediated dUTP nick-end labeling (TUNEL) kit (La Roche Biochemicals) according to the supplier's instructions (24). Immunohistochemical examination was performed by the standard avidin-biotin-peroxidase complex method (ABC Staining System; Santa Cruz Biotechnologies) (24,32) using primary anti-CAT polyclonal antibody (1:500 dilution), anti-cleaved caspase-3 polyclonal antibody (1:50 dilution), anti-collagen type IV monoclonal antibody (1:50 dilution), or anti-Bax polyclonal antibody (1:50 dilution). Targeted proteins were visualized by color development with 3,3′-diaminobenzidine tetrahydrochloride and counterstained with hematoxylin.

The percentage of RPTCs that stained positive on TUNEL assay and active caspase-3 and Bax immunostaining was estimated quantitatively as previously described (24). Briefly, five to six fields (~500–600 cells/field) were randomly selected for each group of animals. The number of RPTCs containing TUNEL-positive active caspase-3 or Bax-staining was divided by the total number of RPTCs counted and multiplied by 100 to calculate the percentage of positively stained RPTCs.

Real-time quantitative PCR assays for gene expression. Total RNA was used in real-time quantitative PCR to quantify the amount of Ang, p53, and Bax mRNA expressed in mRPTs as described previously (24). The forward and reverse primers corresponding to ANG (NM_007428, forward: 5′-ACAGACACCGAGATGCTGTT-3′ and reverse: 5′-CCACGCTCTCTGGATTTATC-3′), p53 (AB020317, forward: 5′ TGATGGAGA GTATTTCACCC-3′ and reverse: 5′-GGGCATCCTTTAACTCTAAG-3′), Bax (L22472, forward: 5′-CTGATCAGAACCATCATGGG-3′ and reverse: 5′-ACAAAGATGGTCACTG TCTG-3′), and β-actin (NM 031144, forward: 5′-ATGCCATCCTGCGTCTGGACCTGGC-3′ and reverse: 5′-AGCATTTGCGGTGCACGATGGAGGG-3′) were used in real-time quantitative PCR assays.

Statistical analysis. Data were expressed as means ± SD. The data were analyzed by one-way ANOVA using Bonferroni correction. $P < 0.05$ was considered statistically significant.

RESULTS

Tissue-specific expression of the KAP2-rCAT transgene in Tg mice. Figure 1*A* presents data from the specific PCR analysis of the rCAT-HA transgene and mutated leptin-receptor gene in offspring of the rCAT-Tg line 688 crossbred with heterozygous db/m$^+$ mice. Animals displaying rCAT-HA transgene and the mutated leptin-receptor gene were used in subsequent experiments.

CAT protein expression in the RPTs of *db/db* rCAT-Tg mice was increased compared with heterozygous db/m$^+$, db/m$^+$ rCAT-Tg and *db/db* mice, respectively (Fig. 1*B*). Enhanced rCAT expression in RPTCs of db/m$^+$ rCAT-Tg and *db/db* rCAT-Tg was documented by immunostaining of CAT in mouse kidneys (Fig. 1*C*). Furthermore, ROS generation was significantly augmented in freshly isolated RPTs from *db/db* mice compared with db/m$^+$ or db/m$^+$

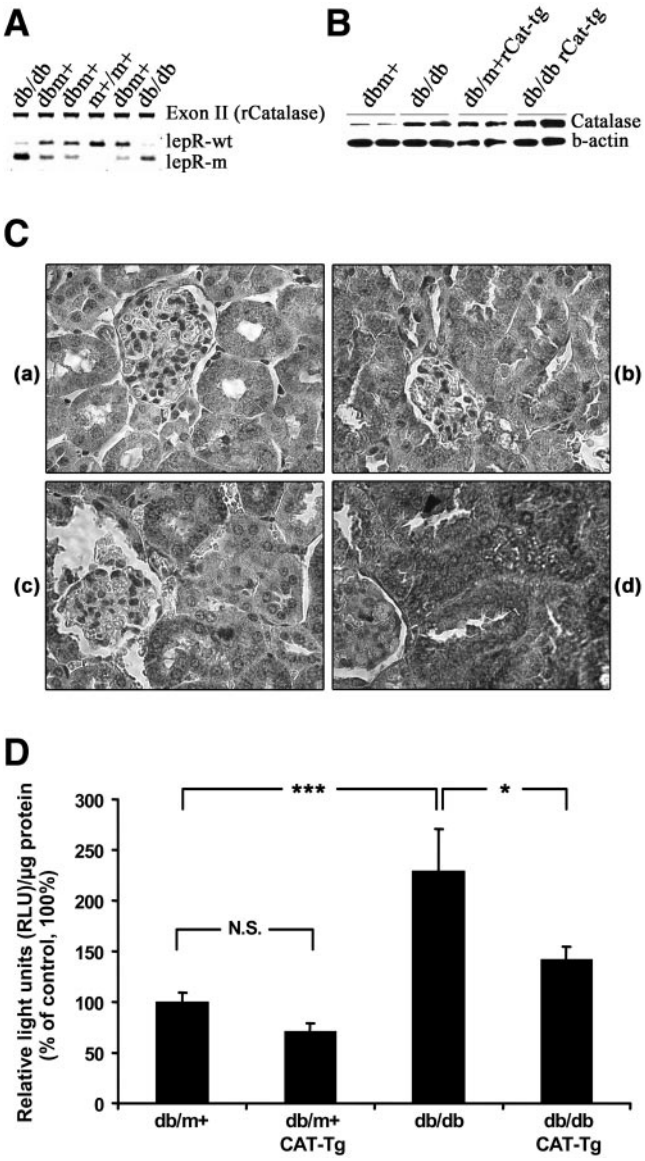

FIG. 1. Generation of Tg mice. *A*: Transgene expression. Specific PCR analysis of rCAT-HA transgene and mutated leptin-receptor gene in offspring of rCAT-Tg line 688 cross-bred with heterozygous db/m$^+$ mice. Animals displaying rCAT-HA transgene and mutated leptin-receptor gene were used in subsequent experiments. *B*: Western blot analysis of rCAT expression in mouse RPT extracts of male non-Tg and Tg mice. *C*: Immunohistochemical staining of CAT in male non-Tg and Tg mouse kidneys, using rabbit anti-CAT polyclonal antibodies. *a*, db/m$^+$ (Lepr-wt) mouse kidney; *b*, db/m$^+$ (Lepr-wt) rCAT-Tg mouse kidney; *c*, *db/db* (Lepr-m) mouse kidney; *d*: *db/db* (Lepr-m) rCAT-Tg mouse kidney. Original magnification ×600. *D*: ROS production in freshly isolated mRPTs. ROS generation in mRPTs were normalized with protein concentration and expressed as relative light units (RLU) per microgram of protein. ROS levels in db/m$^+$ mice were considered as 100%. Each point represents the mean ± SD of six animals (*$P < 0.05$, ***$P < 0.001$; N.S., not significant).

rCAT-Tg mice (Fig. 1*D*). In contrast, the ROS level was significantly attenuated in RPTs of *db/db* rCAT-Tg mice compared with *db/db* mice. Taken together, these results confirm that KAP2 directs rCAT transgene expression in RPTCs of *db/db* rCAT-Tg mice.

Physiological parameters in Tg mice. Body weights (Fig. 2*A*) and blood glucose levels (Fig. 2*B*) of male and female *db/db* and *db/db* rCAT-Tg mice were significantly higher than in db/m$^+$ and db/m$^+$ rCAT-Tg mice, respectively. Body weight and blood glucose level did not differ significantly in nondiabetic db/m$^+$ and db/m$^+$ rCAT-Tg mice or in *db/db* and *db/db* rCAT-Tg mice. Blood glucose in female *db/db* rCAT-Tg mice appeared to be somewhat lower than in female *db/db* mice, but the difference did not reach statistical significance. These results indicate that rCAT overexpression in RPTCs alone is not effective in preventing body weight gain and hyperglycemia in *db/db* mice.

Average systolic blood pressure was increased in both male and female *db/db* mice, from week 10, compared with db/m$^+$ mice, but the differences did not become statistically significant until weeks 12 and 14 in male and female *db/db* mice, respectively (Fig. 3*A*). In contrast, blood pressure remained unchanged in male and female *db/db* rCAT-Tg mice and in db/m$^+$ and db/m$^+$ rCAT-Tg mice (Fig. 3*A*).

Slight increases in the 24-h urinary albumin-to-creatinine ratio were detectable in both male and female *db/db* and *db/db* rCAT-Tg mice after week 16 compared with db/m$^+$ and db/m$^+$ rCAT-Tg mice, respectively (Fig. 3*B*). However, the albumin-to-creatinine ratio at week 16 did not differ significantly in both male and female *db/db* and *db/db* rCAT-Tg. In sharp contrast, the 24-h urinary albumin-to-creatinine ratio was significantly decreased ($P \leq 0.05$) at 18 weeks in both male and female *db/db* rCAT-Tg mice compared with *db/db* mice. These results indicate that rCAT overexpression in RPTCs effectively prevented hypertension development and albuminuria progression in *db/db* mice.

Histological studies. As expected, male db/m$^+$ (Fig. 4*A*, *a* and *e*) and db/m$^+$ rCAT-Tg mice (Fig. 4*A*, *b* and *f*) had normal kidney morphology. However, *db/db* mouse kidneys (Fig. 4*A*, *c* and *g*) displayed cellular edema, reabsorption of droplets, and hypertrophy of glomerular and proximal tubular cell compared with db/m$^+$ mice. Massive inflammatory cell infiltration was also seen in the Bowman's capsule of glomeruli in *db/db* mice. On the other hand, *db/db* rCAT-Tg mice (Fig. 4*A*, *d* and *h*) exhibited glomerular hypertrophy and a milder inflammatory cell infiltration. Moreover, extracellular matrix (ECM) protein expression was increased in *db/db* mouse kidneys compared with those of db/m$^+$ and db/m$^+$ rCAT-Tg and was normalized in *db/db* rCAT-Tg mice. V_G were significantly increased in *db/db* mice compared with db/m$^+$ or db/m$^+$ rCAT-Tg mice. The V_G values in *db/db* rCAT-Tg mice appeared to be slightly larger than in *db/db* mice but did not reach statistical significance (Fig. 4*B*).

Likewise, Masson's trichrome staining and immunostaining revealed, respectively, enhanced expression of collagenous components (Fig. 5*A*) and immunoreactive collagen type IV (Fig. 5*B*) in *db/db* mouse kidneys compared with db/m$^+$ and db/m$^+$ rCAT-Tg. Once again, staining for collagenous components and immunostaining for collagen type IV were normalized in *db/db* rCAT-Tg mouse kidneys, indicating that rCAT overexpression in RPTCs effectively prevented interstitial fibrosis in *db/db* mice.

rCAT overexpression prevents apoptosis In *db/db* mouse RPTs. Next, we investigated whether CAT overexpression could prevent apoptosis induced by hyperglycemia in mouse RPTCs. The TUNEL assay disclosed positively stained nuclei in RPTCs of *db/db* mice (Fig. 6*A*, *c* and *g*) but not in RPTCs of db/m$^+$ mice (Fig. 6*A*, *a* and *e*), db/m$^+$ rCAT-Tg (Fig. 6*A*, *b* and *f*) or *db/db* rCAT-Tg mice (Fig. 6*A*, *e* and *h*). The percentage of the TUNEL-positive RPTCs was significantly higher in *db/db* compared with db/m$^+$ and db/m$^+$ rCAT-Tg mice (Fig. 6*B*). In contrast, the

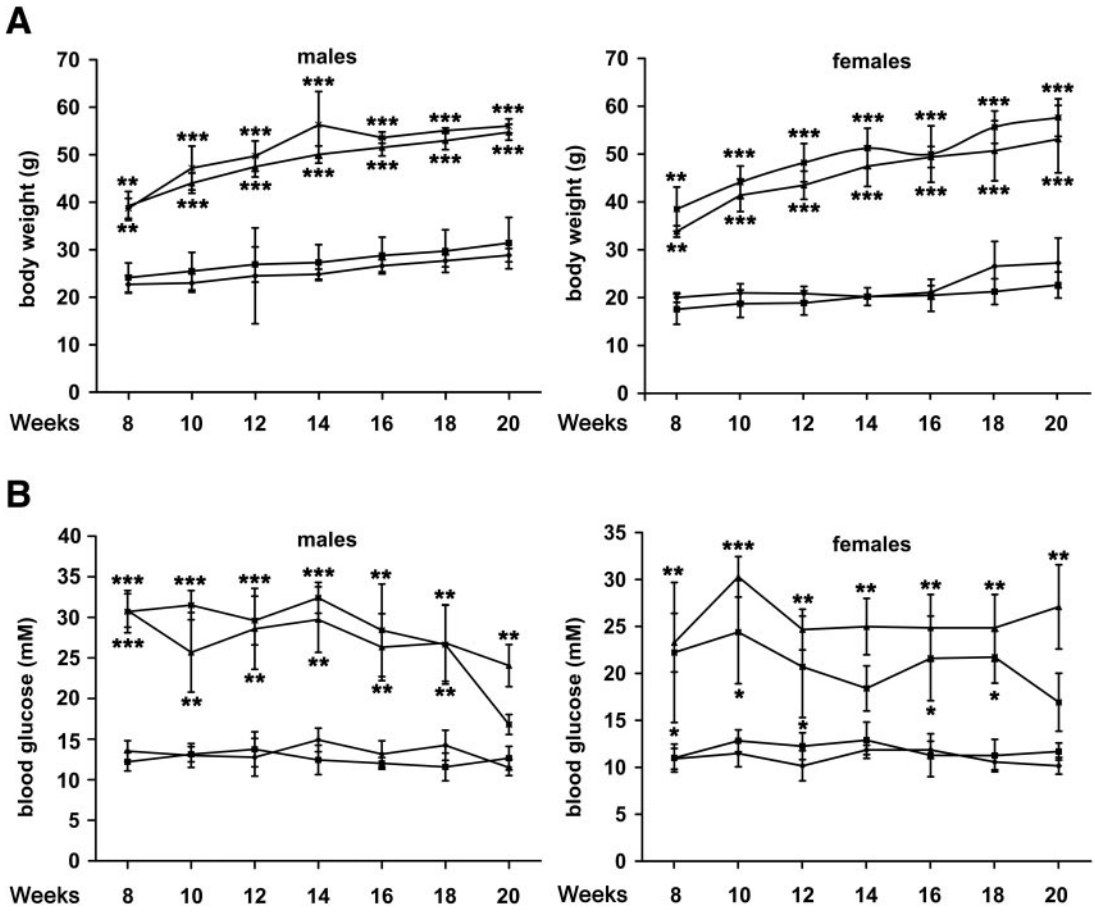

FIG. 2. Changes in mean body weight (*A*) and mean blood glucose (*B*) in male and female non-Tg and Tg mice from weeks 8 to 20. ○, db/m$^+$ mice; □, db/m$^+$ rCAT-Tg mice; ●, *db/db* mice; ■, *db/db* rCAT-Tg mice. The significant difference between *db/db* and db/m$^+$ mice and between *db/db* rCAT-Tg and db/m$^+$ rCAT-Tg mice was calculated (P* < 0.05; ***P* < 0.01; ****P* < 0.005). Values are expressed as means ± SD, *n* = 6 males and 8 females.**

number of TUNEL-positive RPTCs was significantly attenuated in *db/db* rCAT-Tg mice compared with *db/db* mice.

Markedly elevated active caspase-3 expression was detected in RPTCs from *db/db* mice (Fig. 7*A*, *c*) but not in db/m$^+$, db/m$^+$ rCAT-Tg, or *db/db* rCAT-Tg mice (Fig. 7*A*, *a*, *b*, and *d*). Bax expression was also enhanced in RPTCs from *db/db* mice (Fig. 7*B*, *g*) but not in db/m$^+$, db/m$^+$ rCAT-Tg, or *db/db* rCAT-Tg mice (Fig. 7*B*, *e*, *f*, and *h*). These data demonstrate that RPTC apoptosis in diabetic *db/db* mice can be attenuated by rCAT overexpression. These observations were confirmed by quantitation of the immunostaining of active caspase-3 and Bax (Fig. 7*C*). Importantly, active caspase-3 and Bax immunostaining were significantly attenuated in *db/db* rCAT-Tg mice. These data demonstrate that rCAT overexpression effectively attenuated RPTC apoptosis in diabetic *db/db* mice.

ANG and proapoptotic gene mRNA expression in mouse RPTs. Expression of ANG mRNA (Fig. 8*A*), Bax mRNA (Fig. 8*B*), and p53 mRNA (Fig. 8*C*) was significantly elevated in RPTs from *db/db* mice compared with db/m$^+$, db/m$^+$ rCAT-Tg, and *db/db* rCAT-Tg mice. These increases were prevented in *db/db* rCAT-Tg mice.

DISCUSSION

We report here that rCAT overexpression in RPTCs of *db/db* mice effectively attenuates hypertension, albuminuria, interstitial fibrosis, tubular apoptosis, and proapoptotic gene expression, demonstrating an important role for ROS in tubular injury in diabetes.

Enhanced formation of ROS induces apoptosis of podocytes and mesangial and tubular cells (6,9,35). To investigate whether CAT can attenuate kidney injury in type 2 diabetic *db/db* mice, we created *db/db* Tg mice overexpressing rCAT specifically in their RPTs. The CAT transgene and the mutated insulin-2 gene were expressed in kidneys of homozygous *db/db* CAT-Tg mice. CAT protein expression (assessed by Western blotting) was at least twofold higher in RPTs from *db/db* CAT-Tg mice compared with db/m$^+$, db/m$^+$ CAT-Tg, or *db/db* mice. Likewise, immunostaining for CAT and ROS generation were higher in RPTCs of *db/db* CAT-Tg mice compared with those of db/m$^+$, db/m$^+$ CAT-Tg, and *db/db* mice. These findings confirm that KAP directs transgene expression in RPTCs (30,32).

The *db/db* mouse (Lepr$^{db/db}$) is a useful animal model to investigate the pathogenesis of nephropathy in type 2 diabetes because the renal lesions in *db/db* mice (BKS.Cg-m$^{+/+}$ background (36,37) and B6.Cg-m$^{+/+}$ background (38), as well as those without background specified (39,40), closely resemble those in human type 2 diabetes. These include albuminuria, mesangial matrix expansion, glomerulosclerosis, glomerular and tubular hypertrophy and apoptosis, and ECM gene expression, as well as macrophage accumulation and activation. In the present

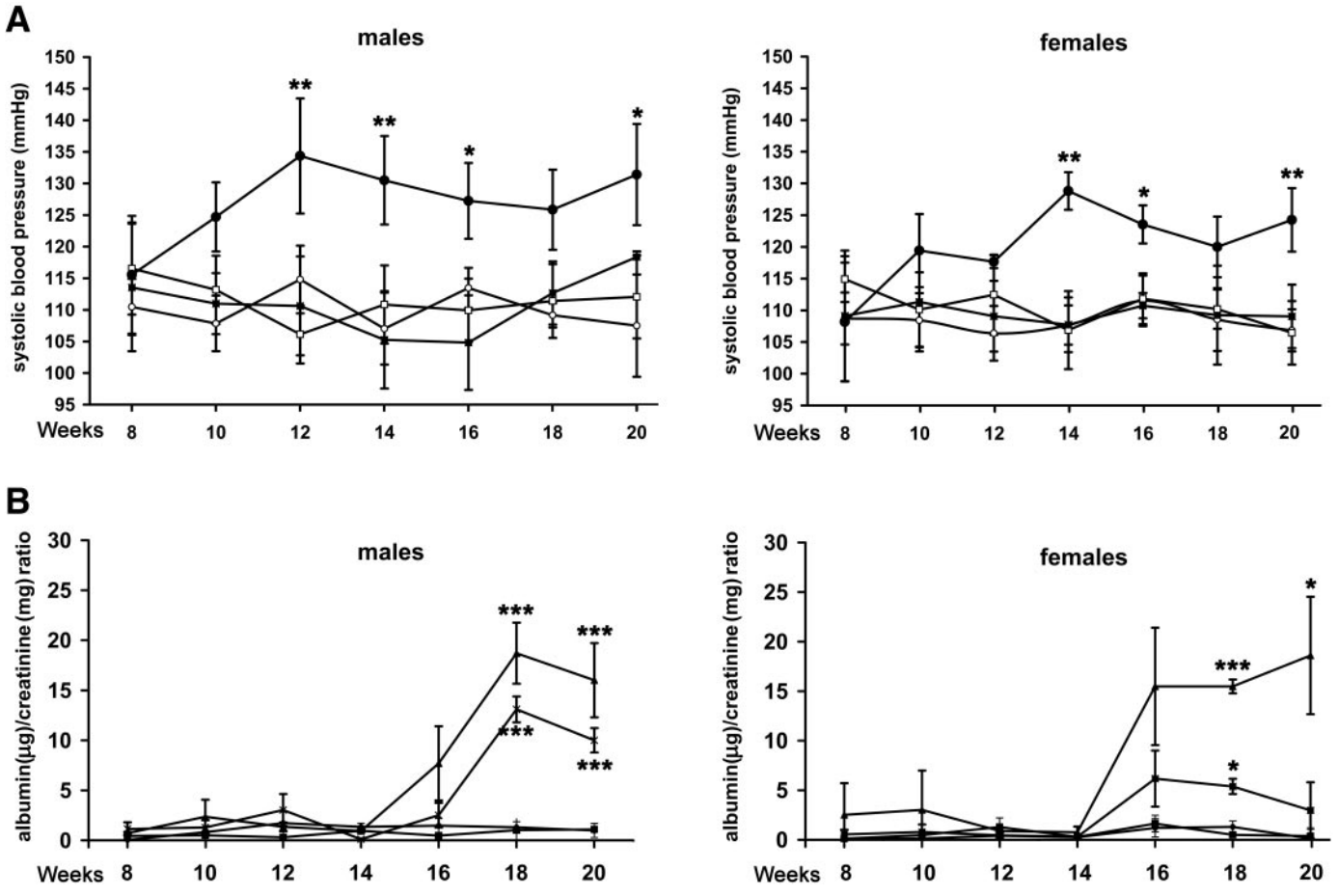

FIG. 3. Changes in mean blood pressure (*A*) and mean albumin (μg)-to-creatinine (mg) ratios (*B*) in male and female non-Tg and Tg mice from 8 to 20 weeks. ○, db/m$^+$ mice; □, db/m$^+$ rCAT-Tg mice; ●, *db/db* mice; ■, *db/db* rCAT-Tg mice. The significant difference between *db/db* and db/m$^+$ mice and between *db/db* rCAT-Tg and db/m$^+$ rCAT-Tg mice was calculated (*$P < 0.05$; **$P < 0.01$; ***$P < 0.005$). Values are expressed as means ± SD, $n = 6$ males and 8 females.

study, we detected increases in body weight and blood glucose level in both male and female *db/db* and *db/db* rCAT-Tg mice in comparison with db/m$^+$ and db/m$^+$ rCAT-Tg mice, respectively. These features are characteristic of *db/db* mice of both backgrounds (36–40).

Longitudinal experiments revealed that baseline blood pressure in both male and female *db/db* mice was significantly higher than in db/m$^+$ and db/m$^+$ rCAT mice. Between weeks 14 and 20, systolic blood pressure of *db/db* mice increased on average by 20–30 mmHg ($P < 0.05$) compared with db/m$^+$ and db/m$^+$ rCAT-Tg mice (average systolic blood pressure in db/m$^+$ and db/m$^+$ rCAT-Tg mice: 100 to 110 mmHg). At the present, we have no explanation for the lack of blood pressure changes in *db/db* mice in another study (36). A possible explanation might be that we have performed longitudinal blood pressure measurement (starting from week 8 to week 20) in the same animals (Fig. 3*A*), as opposed to cross-sectional blood pressure measurements in previous studies.

Interestingly, systolic blood pressure was normalized in *db/db* rCAT-Tg mice as compared with *db/db* mice, indicating that attenuation of ROS generation by CAT can prevent development of hypertension in *db/db* mice. At present, little is known about the mechanisms that lead to elevated blood pressure in *db/db*. One possibility is that enhanced intrarenal RAS activation may underlie the increases in blood pressure. Indeed, we have previously reported that Tg mice overexpressing ANG in their RPTCs do develop hypertension (32). Furthermore, our present data show that ANG mRNA expression is threefold higher in RPTs from *db/db* mice than in db/m$^+$ mice and is normalized in *db/db* rCAT-Tg mice.

Since microalbuminuria is an important clinical marker for the early detection of hypertension- or diabetes-induced nephropathy, we monitored urinary albuminuria using the albumin-to-creatinine ratio. Albuminuria was detectable only after week 16 in *db/db* and db/m$^+$ rCAT-Tg mice. In male *db/db* mice, albuminuria increased further at week 18 to levels comparable with those in female *db/db* mice at week 16. rCAT overexpression in *db/db* rCAT-Tg mice significantly ($P \leq 0.05$) reduced albuminuria in both male and female mice at weeks 18 and 20 compared with *db/db* mice. To our best knowledge, this is the first report that rCAT overexpression in RPTCs can effectively attenuate the development of hypertension and progression of albuminuria in both male and female *db/db* mice. Overexpression of rCAT in female *db/db* mice was, however, more effective in lowering the albumin-to-creatinine ratio than in male *db/db* mice. This may be explained by differences in the effect of exogenous and endogenous testosterone on the kidney-specific androgen-regulated protein (KAP2) promoter, which controls the expression of the rCAT-HA transgene in Tg mice and is regulated by blood testosterone levels. In female Tg mice, testosterone pellets were implanted to stimulate the rCAT-HA expression in the kidney chronically. Since male Tg mice were implanted

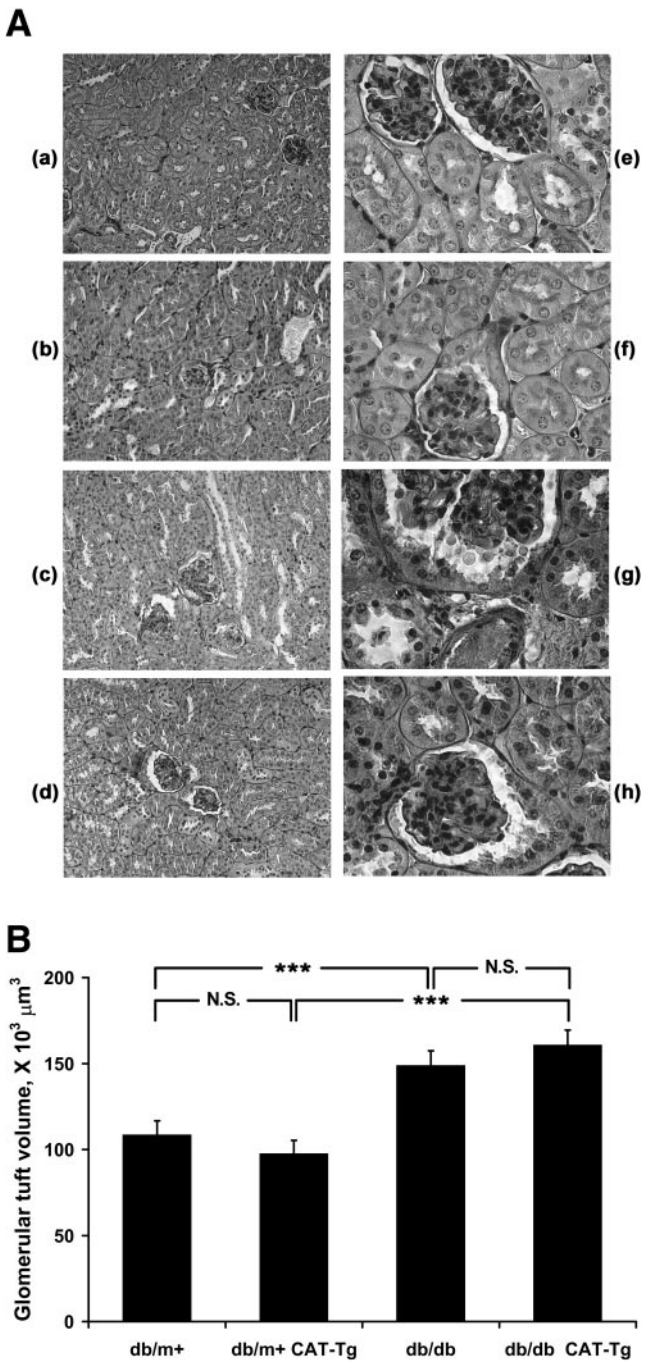

FIG. 4. Periodic-acid Schiff staining of male non-Tg and Tg mouse kidneys at week 20. *A*: *a* and *e*, db/m$^+$ control littermate; *b* and *f*, db/m$^+$ rCAT-Tg mouse; *c* and *g*, *db/db* mouse; *d* and *h*, *db/db* rCAT-Tg mouse. *a*, *b*, *c*, and *d*, original magnification ×100. *e*, *f*, *g*, and *h*, original magnification ×600. *B*: Quantitation of mean glomerular volume (V_G) of male non-Tg and Tg mouse kidneys at week 20 (*$P < 0.005$; N.S., not significant). Values are expressed as means ± SE, $n = 6$ males.**

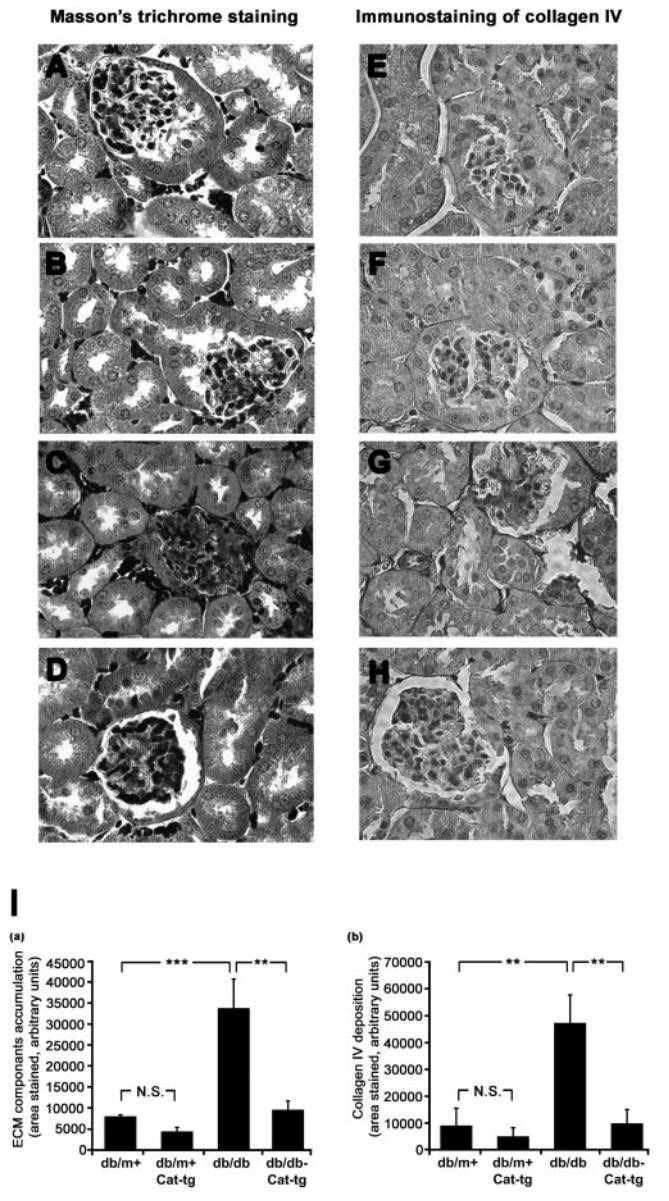

FIG. 5. Masson's trichrome staining (*A–D*) and immunostaining for collagen IV (*E–H*) in male non-Tg and Tg mouse kidneys at week 20. *A* and *E*, db/m$^+$ control littermate; *B* and *F*, db/m$^+$ rCAT-Tg mouse; *C* and *G*, *db/db* mouse; *D* and *H*, *db/db* rCAT-Tg mouse. Original magnification × 600. *I*: Quantification of ECM components accumulation (Masson's trichrome staining) (*a*) and collagen IV deposition (*b*).

with placebo pellets, the rCAT-HA expression is regulated by endogenous blood testosterone level that shows interindividual variation. Hence, the response in testosterone-treated female Tg mice would be more marked as compared with male Tg mice. Taken together, these observations imply a link between renal ROS generation, hypertension, and albuminuria. However, it remains to be investigated whether albuminuria is secondary to elevated blood pressure, whether hypertension and albuminuria are unrelated events, and/or whether enhanced intrarenal ROS generation alone is capable of inducing albuminuria independently of systemic hypertension.

Histological examinations confirmed the presence of characteristic features of renal injury in the kidneys of *db/db* mice (36). In contrast, *db/db* rCAT-Tg mice exhibited glomerular hypertrophy, a milder inflammatory cell infiltration, and renal histology similar to that of db/m$^+$ rCAT-Tg mice. Furthermore, ECM protein and collagen expression were attenuated in the kidneys of *db/db* rCAT-Tg mice. By using immunostaining, we also detected enhanced collagen type IV expression in glomeruli and tubulointerstitial spaces in *db/db* mice. Surprisingly, collagen type IV expression was completely normalized in *db/db* rCAT-Tg compared with db/m$^+$ and db/m$^+$ rCAT-Tg mice. These data suggest a critical role for tubular ROS generation in the development of interstitial fibrosis in diabetic *db/db* mice.

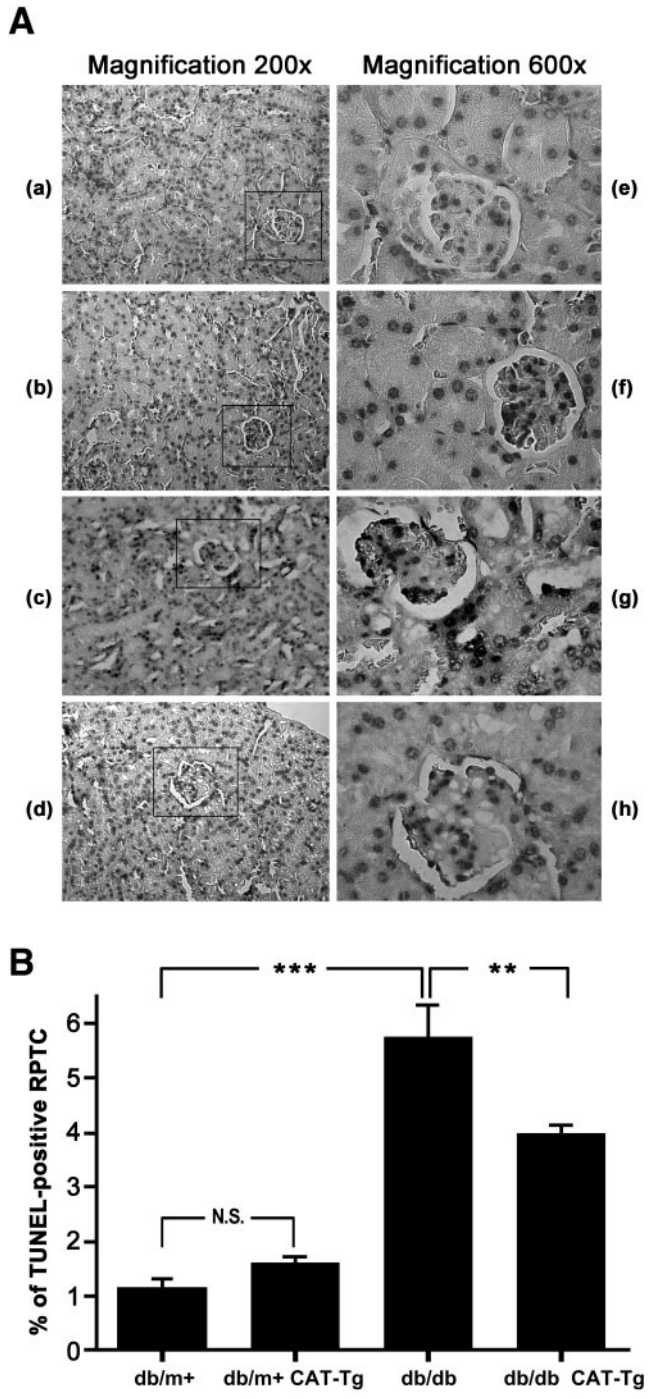

FIG. 6. Apoptosis in male non-Tg and Tg mouse kidneys at week 20, analyzed by TUNEL staining. *A*) *a* and *e*, db/m$^+$ control littermate; *b* and *f*, db/m$^+$ rCAT-Tg mouse; *c* and *g*, *db/db* mouse; *d* and *h*, *db/db* rCAT-Tg mouse. *a–d*, original magnification ×200. *e–h*, original magnification ×600. Arrow heads indicate apoptotic cells in proximal tubules. *B*: Bar graph showing quantitative analysis of TUNEL-positive stained RPTCs from male non-Tg and Tg mouse kidneys at week 20. All data are expressed as means ± SD, *n* = 6 (P* < 0.05; N.S., not significant).**

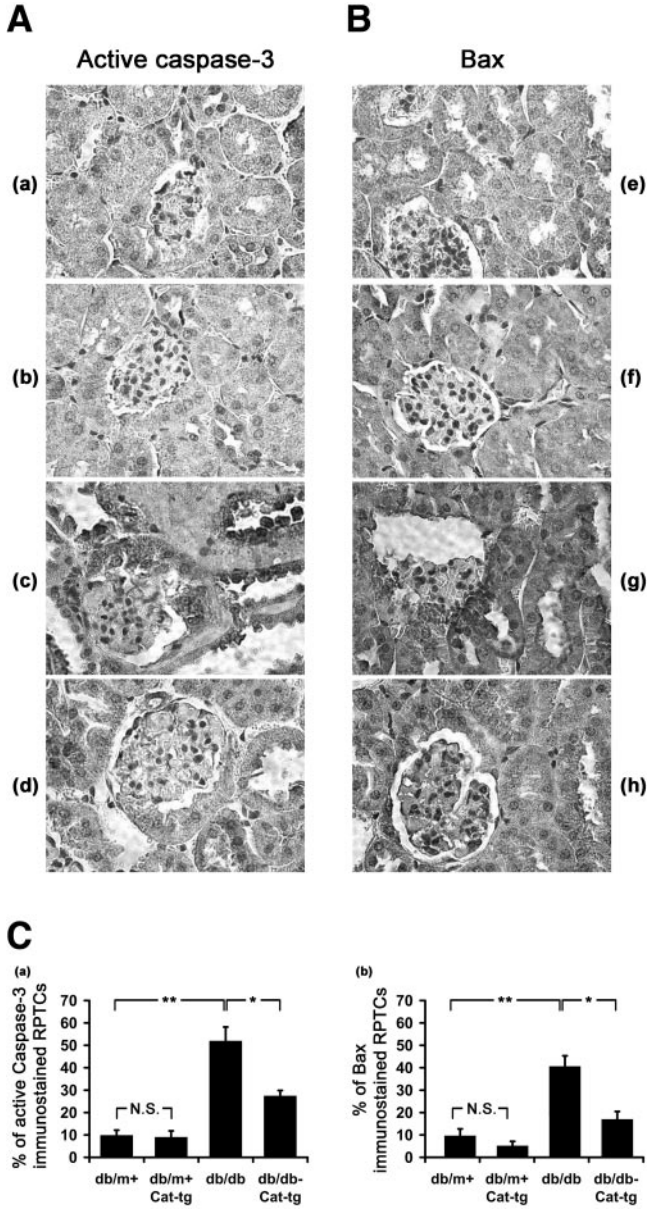

FIG. 7. Immunohistochemical staining of α-active caspase-3 and Bax in male non-Tg and Tg mouse kidneys at week 20, using rabbit anti–α-active caspase-3 and anti-Bax polyclonal antibodies, respectively. *A*: α-active caspase-3 immunostaining (*a–d*). *B*: Bax immunostaining (*e–h*). *a* and *e*, db/m$^+$ control littermate; *b* and *f*, db/m$^+$ rCAT-Tg mouse; *c* and *g*, *db/db* mouse; *d* and *h*, *db/db* rCAT-Tg mouse. Original magnification ×600. *C*: Quantitative analysis of active caspase-3 and Bax-positive RPTCs from male non-Tg and Tg mouse kidneys at week 20. Immunostained active caspase-3 (*a*) and Bax (*b*). All data are expressed as means ± SD, *n* = 6 (P* < 0.05; N.S., not significant).**

High glucose is a potent inducer of apoptosis in RPTCs via ROS generation (6,9). Consistently, we detected significantly higher number of apoptotic cells in RPTs of diabetic *db/db* mice than in RPTCs of db/m$^+$ or db/m$^+$ rCAT-Tg mice, whereas apoptosis was significantly reduced in *db/db* rCAT-Tg mice. These observations indicate that ROS generation in RPTCs of *db/db* mice actually induces tubular apoptosis and that CAT overexpression can at least partially prevent it. Indeed, active caspase-3 and Bax expression was normalized in *db/db* rCAT-Tg mice. Furthermore, RPTs from *db/db* mice exhibited markedly elevated expression of the proapoptotic genes p53 and Bax. Our observations that Bax and p53 mRNA expression was considerably lower in *db/db* rCAT-Tg mice than in *db/db* mice lend further support to the concept that rCAT overexpression attenuates RPTC apoptosis in *db/db* mice.

The precise mechanism(s) by which ROS cause hypertension and tubular injury (albuminuria, interstitial fibrosis, and RPTC apoptosis) in *db/db* mice remains unclear. One possibility is that ROS stimulate ANG production and

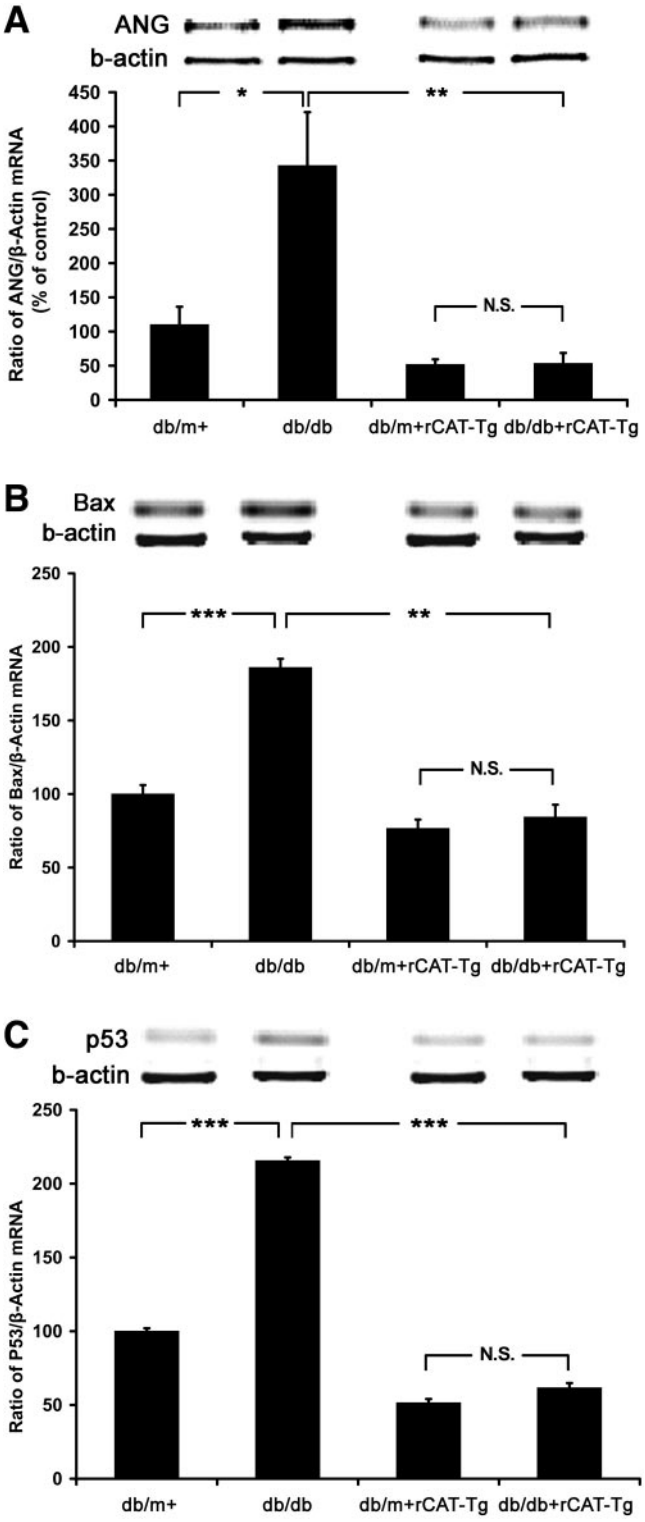

FIG. 8. Expression of Ang, Bax, and p53 mRNA in RPTs of non-Tg and Tg mice quantified by real-time quantitative PCR at week 20. RPTs from non-Tg and Tg mice were isolated and assayed for ANG (*A*), Bax (*B*) and p53 (*C*) mRNA. The relative densities of ANG, Bax, and p53 mRNA were normalized with β-actin mRNA control. ANG, Bax, and p53 mRNA levels in db/m$^+$ mice were considered as 100%. Each point represents the mean ± SD of six animals (P* < 0.05, ***P* < 0.01; N.S., not significant).**

activate the intrarenal RAS as RPTCs express all RAS components (41). Ang II promotes sodium reabsorption via stimulation of sodium/hydrogen exchanger activity in RPTCs (42), ultimately leading to development of hypertension. Furthermore, Ang II is capable of stimulating transforming growth factor-β 1 (TGF-β1) and subsequently enhancing ECM protein, collagen type IV, and proapoptotic genes in RPTCs, leading to tubular injury (interstitial fibrosis and cellular apoptosis) (43). Indeed, neutralization of TGF-β alleviated fibrosis in diabetic animal models, including *db/db* mice (44). Moreover, TGF-β1 was reported to promote apoptosis after renal injury in both in vivo and in vitro models (45,46). We have previously found that intrarenal ANG gene expression is essential for TGF-β1 gene expression in rat RPTCs exposed to high glucose in vitro (47) and that Tg mice overexpressing ANG in RPTCs exhibit hypertension and albuminuria (32). Our present data showed at least threefold higher ANG mRNA expression in RPTs of *db/db* mice and normalization of ANG mRNA expression in *db/db* rCAT-Tg mice. Taken together, these findings support a role for intrarenal ROS and RAS in the induction of interstitial fibrosis and RPTC apoptosis.

The present results may have clinical implications to type 2 diabetes. Since tubular apoptosis is detectable in human diabetic kidneys with albuminuria (27,28), and tubular atrophy appears to be a better indicator of disease progression than glomerular pathology (13–18), we suggest that RPTC apoptosis may be an initial mechanism for tubular atrophy in diabetes. Our data point toward ROS as one of the key mediators of this process. The source(s) of ROS production in RPTs remains, however, to be identified. Among these sources, mitochondrial (29) and membrane-bound NADPH oxidase-derived (48) ROS production have already been reported. Interestingly, diabetes is associated with enhanced expression of NADPH oxidase subunits, Nox2, Nox4, and p47^{phox} mRNA and p47^{phox} in mouse glomeruli (49), indicating that these NADPH oxidase subunits might be involved in ROS production in RPTs. Clearly, more experiments along these lines are warranted.

In summary, the present study suggest a critical role for CAT in attenuating hypertension, albuminuria, interstitial fibrosis, and RPTC apoptosis in *db/db* mice in vivo. Our studies raise the possibility that selective activation of this enzyme may provide a novel approach in preventing or reversing the pathophysiological manifestations of diabetic nephropathy including tubular atrophy in type 2 diabetes.

ACKNOWLEDGMENTS

This work was supported by a grant from the Canadian Institutes of Health Research (MOP 62920 to J.S.D.C.), the Kidney Foundation of Canada, and the U.S. National Institutes of Health (HL-48455 to J.R.I.).

The authors thank Dr. Paul Goodyer (Montreal Children's Hospital, MUHC, Montreal, QC, Canada) for advice on the quantitation of the glomerular volume and Mr. Ovid M. Da Silva, Editor, Research Support Office, Research Centre, CHUM, for editing this manuscript.

REFERENCES

1. United States Renal Data System: *USRDS Annual Data Report*. Bethesda, MD, National Institutes of Health, National Institute of Diabetes and Digestive and Kidney Diseases, 2005
2. American Diabetes Association: Nephropathy in diabetes (Position Statement). *Diabetes Care* 27 (Suppl. 1):S79–S83, 2004
3. Jensen T, Borch-Johnsen K, Kofoed-Enevoldsen A, Deckert T: Coronary artery disease in young type 1 (insulin-dependent) diabetic patients with

and without diabetic nephropathy: incidence and risk factors. *Diabetologica* 30:144–148, 1987
4. Wolf G: New insights into the pathophysiology of diabetic nephropathy: from haemodynamics to molecular pathology. *Eur J Clin Invest* 34:785–796, 2004
5. Ha H, Lee HB: Reactive oxygen species as glucose signaling molecules in mesangial cells cultured under high glucose. *Kidney Int* 58 (Suppl. 77):S19–S25, 2000
6. Kang BP, Frencher S, Reddy V, Kessler A, Malhotta A, Meggs LG: High glucose promotes mesangial cell apoptosis by oxidant-dependent mechanism. *Am J Physiol* 284:F455–F466, 2003
7. Allen DA, Harwood S, Varagunam M, Raftery MJ, Yaqoob MM: High glucose-induced oxidative stress causes apoptosis in proximal tubular epithelial cells and is mediated by multiple caspases. *FASEB J* 17:908–910, 2003
8. James EA, Galceran JM, Raij L: Angiotensin II induces superoxide anion production by mesangial cells. *Kidney Int* 54:775–784, 1998
9. Haugen EN, Croatt AJ, Nath KA: Angiotensin II induces renal oxidant stress in vivo and heme oxygenase-1 in vivo and in vitro. *Kidney Int* 58:144–152, 2000
10. Wolf G: Free radical production and angiotensin. *Curr Hypertens Rep* 2:167–173, 2000
11. Seshiah PN, Weber DS, Racic P, Valppu L, Tanujama Y, Griendling KK: Angiotensin II stimulation of NAD(P)H oxidase activity: upstream mediators. *Circ Res* 91:406–413, 2002
12. Najafian B, Kim Y, Crosson JT, Mauer M: Atubular glomeruli and glomerulotubular junction abnormalities in diabetic nephropathy. *J Am Soc Nephrol* 14:908–917, 2003
13. Najafian B, Crosson JT, Kim Y, Mauer M: Glomerulotubular junction abnormalities are associated with proteinuria in type 1 diabetes. *J Am Soc Nephrol* 17:S53–S60, 2006
14. Lindop GBM, Gibson IW, Downie TT, Vass D, Cohen EP: The glomerulotubular junction: a target in renal disease (Review). *J Pathol* 197:1–3, 2002
15. Marcussen N: Tubulointerstitial damage leads to atubular glomeruli: significance and possible role in progression. *Nephrol Dial Transplant* 15 (Suppl. 6):74–75, 2000
16. Gilbert RE, Cooper ME: The tubulointerstitium in progressive diabetic kidney disease: more than an aftermath of glomerular injury? *Kidney Int* 56:1627–1637, 1999
17. Eddy AA: Molecular basis of renal fibrosis. *Pediatr Nephrol* 15:290–301, 2000
18. Sugiyama M, Kashihara N, Makino H, Yamasaki Y, Ota Z: Apoptosis in glomerular sclerosis. *Kidney Int* 49:103–111, 1996
19. Woo D: Apoptosis and loss of renal tissue in polycystic kidney diseases. *N Engl J Med* 333:18–25, 1995
20. Schumer M, Colombel MC, Sawczuk IS, Gobe G, Connor J, O'Toole KM, Olsson CA, Wise GJ, Buttiyan R: Morphologic, biochemical, and molecular evidence of apoptosis during reperfusion phase after brief periods of renal ischemia. *Am J Pathol* 140:831–838, 1992
21. Justo P, Lorez C, Sanz A, Egido J, Ortiz A: Intracellular mechanisms of cyclosporine A-induced tubular cell apoptosis. *J Am Soc Nephrol* 14:3072–3080, 2003
22. de Haan JB, Stefanovic N, Nikolic-Paterson D, Scurr LL, Croft KD, Mori TA, Hertzog P, Kola I, Atkins RC, Tesch GH: Kidney expression of glutathione peroxidase-1 is not protective against streptozotocin-induced diabetic nephropathy. *Am J Physiol Renal Physiol* 289:F544–F551, 2005
23. Zhang Y, Wada J, Hashimoto I, Eguchi J, Yasuhara A, Kanwar YS, Shikata K, Makino H: Therapeutic approach for diabetic nephropathy using gene delivery of translocase of inner mitochondrial membrane 44 by reducing mitochondrial superoxide production. *J Am Soc Nephrol* 17:1090–1101, 2006
24. Brezniceanu M-L, Liu L, Zhang S-L, Sachetelli S, Guo D-F, Filep JG, Ingelfinger JR, Chan JSD: Attenuation of angiotensinogen gene expression and apoptosis in proximal tubular cells of catalase transgenic mice. *Kidney Int* 71:912–923, 2007
25. Kumar D, Zimpelmann J, Robertson S, Burns KD: Tubular and interstitial cell apoptosis in the streptozotocin-diabetic rat kidney. *Nephron Exp Nephrol* 96:e77–e88, 2004
26. Kelly DJ, Stein-Oakley A, Zhang Y, Wassef L, Maguire J, Koji T, Thomson N, Wilkinson-Berka JL, Gilbert RE: Fas-induced apoptosis is a feature of progressive diabetic nephropathy in transgenic (mRen-2)27 rats: attenuation with renin-angiotensin blockade. *Nephrology (Carlton)* 9:7–13, 2004
27. Kumar D, Robertson S, Burns KD: Evidence of apoptosis in human diabetic kidney. *Mol Cell Biochem* 259:67–70, 2004
28. Susztak K, Ciccone E, McCue P, Sharma K, Bottinger EP: Multiple metabolic hits converge on CD36 as novel mediator of tubular epithelial apoptosis in diabetic nephropathy. *PLoS Med* 2:e45, 2005
29. Hsieh T-J, Zhang S-L, Filep JG, Tang S-S, Ingelfinger JR, Chan JSD: High glucose stimulates angiotensinogen gene expression via reactive oxygen species (ROS) generation in rat kidney proximal tubular cells. *Endocrinology* 143:2975–2985, 2002
30. Ding Y, Sigmund CD: Androgen-dependent regulation of human angiotensinogen expression in KAP-hAGT transgenic mice. *Am J Physiol Renal Physiol* 280:F54–F60, 2001
31. Schreyer SA, Chua Sc Jr, LeBoeuf RC: Obesity and diabetes in a TNF-alpha receptor-deficient mice. *J Clin Invest* 102:402–411, 1998
32. Sachetelli S, Liu Q, Zhang S-L, Liu F, Hsieh T-J, Brezniceanu M-J, Guo D-F, Ingelfinger JR, Chan JSD: RAS blockade decreases blood pressure and proteinuria in transgenic mice overexpressing rat angiotensinogen gene in the kidney. *Kidney Int* 69:1016–1023, 2006
33. Brezniceanu M-L, Wei C-C, Zhang S-L, Hsieh T-J, Guo D-F, Hébert M-J, Ingelfinger JR, Filep JA, Chan JSD.: Transforming growth factor-beta 1 stimulates angiotensinogen gene expression in kidney proximal tubular cells. *Kidney Int* 69:1977–1985, 2006
34. Weibel ER: Numerical density: shape and size of particles. In *Sterological Methods*. Vol. 2, *Theoretical Foundations*. Weibel ER, Ed. London, Academic Press, 1980, p. 149–152,
35. Susztak K, Raff AC, Schiffer M, Bottinger EP: Glucose-induced reactive oxygen species cause apoptosis of podocytes and podocyte depletion at the onset of diabetic nephropathy. *Diabetes* 55:225–233, 2006
36. Sharma K, McCue P, Dunn SR: Diabetic kidney disease in the db/db mouse. *Am J Physiol Renal Physiol* 284:F1138–F1144, 2003
37. Sugaru E, Nakagawa T, Ono-Kishino M, Nagamine J, Tikunaga T, Kitoh M, Hume WE, Nagata R, Taiji M: Amelioration of established diabetic nephropathy by combined treatment with SMP-534 (antifibrotic agent) and losartan in db/db mice. *Nephron Exp Nephrol* 105:e45–e52, 2006
38. Zheng F, Cornacchia F, Schulman I, Banerjee A, Cheng QL, Potier M, Plati AR, Berbo M, Elliot SJ, Li J, Fornoni A, Zang YJ, Zisman A, Striker LJ, Striker CE: Development of albuminuria and glomerular lesions in normoglycemic B6 recipients of db/db mice bone marrow: the role of mesangial cell progenitors. *Diabetes* 53:2420–2427, 2004
39. Cohen MP, Lautenslager CT, Sherman CW: Increased urinary type IV collagen marks the development of glomerular pathology in diabetic db/db mice. *Metabolism* 50:1435–1440, 2001
40. Koya D, Haneda M, Nakagawa H, Isshiki K, Sato H, Maeda S, Sugimoto T, Yasuda H, Kashiwagi A, Ways DK, King GL, Kikkawa R: Amelioration of accelerated diabetic mesagial expansion by treatment with a PKC beta inhibitor in diabetic db/db mice, a rodent model for type 2 diabetes. *FASEB J* 14:439–447, 2000
41. Tang S-S, Jung F, Diamant D, Brown D, Bachinsky D, Hellman P, Ingelfinger JR: Temperature-sensitive SV40 immortalized rat proximal tubule cell line has functional renin-angiotensin system. *Am J Physiol* 268:F435–F446, 1995
42. Saccomani G, Mitchell KD, Navar LG: Angiotensin II stimulation of Na^+-H^+ exchange in proximal tubule cells. *Am J Physiol Renal Physiol* 258:F1188–F1195, 1990
43. Roberts AB, McCune BK, Sporn MB: TGF-β: regulation of extracellular matrix. *Kidney Int* 41:557–559, 1992
44. Ziyadeh FN, Hoffman BB, Han DC, Iglesias-De La Cruz MC, Hong SW, Isono M, Chen S, McGowan TA, Sharma K: Long-term prevention of renal insufficiency, excess matrix gene expression, and glomerular mesangial matrix expression by treatment with monoclonal antitransforming growth factor-β antibody in db/db diabetic mice. *Proc Natl Acad Sci USA* 97:8015–8020, 2000
45. Dai C, Yang J, Liu Y: Transforming growth factor-β1 potentiates renal tubular epithelial cell death by a mechanism independent of Smad signalling. *J Biol Chem* 278:12537–12545, 2003
46. Miyalima A, Chen J, Lawence C, Ledbetter S, Soslow RA, Stern J, Jha S, Pigato J, Lemer ML, Poppas DP, Vaughan ED, Felsen D: Antibody to transforming growth factor-β ameliorates tubular apoptosis in unilateral ureteral obstruction. *Kidney Int* 58:2301–2313, 2000
47. Zhang S-L., To C, Chen X, Filep JG, Tang S-S, Ingelfinger JR, Chan JSD: Essential role(s) of the intrarenal renin-angiotensin system in transforming growth factor-β1 gene expression and induction of hypertrophy in rat kidney proximal tubular cells in high glucose. *J Am Soc Nephrol* 13:302–312, 2002
48. Hsieh T-J, Fustier P, Wei C-C, Zhang S-L, Filep JG, Tang S-S, Ingelfinger JR, Fantus IG, Hamet P, Chan JSD: Reactive oxygen species blockade and insulin action on angiotensinogen gene expression in proximal tubular cells. *J Endocrinol* 183:535–550, 2004
49. Ohshiro Y, Ma RC, Yasuda Y, Hiraoka-Yamamoto J, Clermont AC, Isshiki K, Yagi K, Arikawa E, Kern TS, King GL: Reduction of diabetes-induced oxidative stress, fibrotic cytokine expression, and renal dysfunction in protein kinase Cβ-null mice. *Diabetes* 55:3112–3120, 2006